

SERENDIPITOUS *XMM-Newton* DISCOVERY OF A CLUSTER OF GALAXIES AT $z = 0.28$ FABIO GASTALDELLO¹, DAVID A. BUOTE¹, PHILIP J. HUMPHREY¹, LUCA ZAPPACOSTA¹, MARC S. SEIGAR¹, AARON J. BARTH¹, FABRIZIO BRIGHENTI^{2,3}, & WILLIAM G. MATHEWS²*Submitted Nov 27, 2006; Accepted March 16, 2007 for publication in the Astrophysical Journal*

ABSTRACT

We report the discovery of a galaxy cluster serendipitously detected as an extended X-ray source in an offset observation of the group NGC 5044. The cluster redshift, $z=0.281$, determined from the optical spectrum of the brightest cluster galaxy, agrees with that inferred from the X-ray spectrum using the Fe K α complex of the hot ICM ($z = 0.27 \pm 0.01$). Based on the 50 ks *XMM* observation, we find that within a radius of 383 kpc the cluster has an unabsorbed X-ray flux, $f_X(0.5 - 2 \text{ keV}) = (3.34^{+0.08}_{-0.13}) \times 10^{-13} \text{ ergs cm}^{-2} \text{ s}^{-1}$, a bolometric X-ray luminosity, $L_X = (2.21^{+0.34}_{-0.19}) \times 10^{44} \text{ ergs s}^{-1}$, $kT = 3.57 \pm 0.12 \text{ keV}$, and metallicity, $0.60 \pm 0.09 Z_\odot$. The cluster obeys the scaling relations for L_X and T observed at intermediate redshift. The mass derived from an isothermal NFW model fit is, $M_{\text{vir}} = 3.89 \pm 0.35 \times 10^{14} M_\odot$, with a concentration parameter, $c = 6.7 \pm 0.4$, consistent with the range of values expected in the concordance cosmological model for relaxed clusters. The optical properties suggest this could be a “fossil cluster”.

Subject headings: galaxies: clusters: general — X-rays: general

1. INTRODUCTION

Galaxy groups and low mass clusters ($T < 4 \text{ keV}$) are starting to be detected and analyzed in detail in the X-ray band at intermediate redshift $0.2 < z < 0.6$ (e.g., Willis et al. 2005; Jeltema et al. 2006). These objects are more likely to display the effects of non-gravitational energy injection into the intracluster medium (ICM) than hotter, more massive, clusters (e.g., Voit 2005). The study of extended X-ray objects over a broad temperature range at $z > 0.2$ will provide important insight into the evolution of their hot gas and the deviation of X-ray scaling relations from simple, self-similar expectations. Studies of objects in the redshift range $0.2 < z < 0.6$ with $kT \sim 2 - 3 \text{ keV}$ already suggest that they are less dynamically evolved than their counterparts at $z = 0$ (Mulchaey et al. 2006).

The combination of surveys specifically designed to detect clusters (e.g. the *XMM-LSS*, Pierre et al. 2004), with serendipitous observations, which can make use of deeper exposures, will further advance the knowledge in this field. Here we present the discovery of a cluster at the redshift of $z = 0.281$, serendipitously observed during an offset observation of the nearby group NGC 5044. All distance-dependent quantities have been computed assuming $H_0 = 70 \text{ km s}^{-1} \text{ Mpc}^{-1}$, $\Omega_m = 0.3$ and $\Omega_\Lambda = 0.7$. At the redshift of $z = 0.281$, $1'$ corresponds to 255 kpc. All the errors quoted are at the 68% confidence limit.

2. X-RAY ANALYSIS

The object XMMU J131359.7–162735 was detected in an offset observation of the group NGC 5044 (obsID 0301290101) performed on 6 January 2006. The source

(see Fig.1) is located at $4.7'$ off-axis, and it is clearly extended on a ~ 2 arc-minute scale. The X-ray centroid of XMMU J131359.7–162735 in equatorial coordinates is $\alpha_{\text{J2000.0}} = 13^{\text{h}}13^{\text{m}}59.7^{\text{s}}$, $\delta_{\text{J2000.0}} = -16^{\circ}27^{\text{m}}35^{\text{s}}$.

The data were reduced with SAS v7.0.0 using the tasks *emchain* and *epchain*. We considered only event patterns 0-12 for MOS and 0 for pn. We cleaned the data using the standard procedures: bright pixels and hot columns were removed by applying the expression *FLAG == 0*, and we corrected for pn out-of-time events. Periods of high background due to soft protons were filtered as in Gastaldello et al. (2006); the observation was very mildly affected by flares leading to only ~ 5 ks of lost data, with net exposures of 52, 50 and 45 ks respectively for MOS1, MOS2 and pn.

For each detector we created images in the 0.5-2 keV band with point sources masked out using circular regions of $25''$ radius centered at each source position. The images have been exposure-corrected, and a radial surface brightness profile was extracted from a circular region of $6'$ radius positioned at the cluster centroid. We account for the X-ray background and the emission of the NGC 5044 group by including a constant background component. The data were grouped to have at least 20 counts per bin in order to apply the χ^2 statistic. The fitted model is folded with the *XMM* PSF at energy of 1 keV. The joint best-fit β model (Cavaliere & Fusco-Femiano 1978) has a core radius of $r_c = 66 \pm 6 \text{ kpc}$ ($15.5'' \pm 1.4''$) and $\beta = 0.54 \pm 0.01$ for $\chi^2/\text{d.o.f.} = 465/273$. Although formally unacceptable, the surface brightness model well-describes the overall shape of the profile, as evinced by the low fractional residuals (see Fig.2). Fits to the profiles of the individual detectors give consistent results within 1σ of the combined-fit result. If we use larger extraction regions, the emission by NGC 5044 can no longer be treated as constant: if we account for the emission of NGC 5044 by adding a second β model at an offset of $20.7'$ (the distance between the source and the emission peak of NGC 5044)

¹ Department of Physics and Astronomy, University of California at Irvine, 4129 Frederick Reines Hall, Irvine, CA 92697-4575

² UCO/Lick Observatory, University of California at Santa Cruz, 1156 High Street, Santa Cruz, CA 95064

³ Dipartimento di Astronomia, Università di Bologna, via Ranzani 1, Bologna 40127, Italy

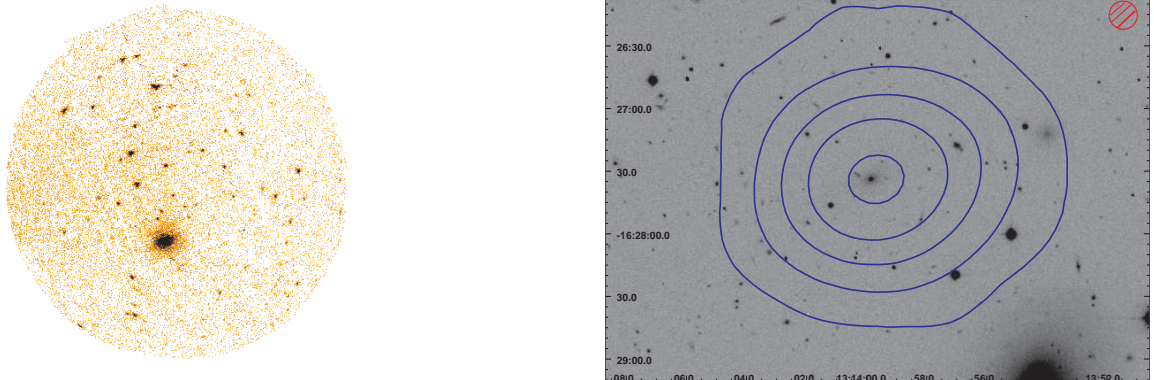


FIG. 1.— *Left*: Exposure corrected 0.5-2.0 keV combined MOS1 and MOS 2 X-ray image of the observed offset field of NGC 5044. The cluster XMMU J131359.7-162735 is clearly visible as the extended source. *Right*: The *V* band image with the smoothed X-ray contours overlaid and logarithmically spaced between 2 and 37 cts/pixel. Coordinates are J2000. The red circle shows the FWHM (6.7'') of the *XMM* MOS PSF at the off-axis angle of the source.

with $r_c = 48''$ and $\beta = 0.53$ (Buote et al. 2003), the resulting parameters for the source are consistent within the 1σ errors.

We extracted spectra for each detector from a 1.5' circular region positioned at the centroid of the emission, chosen to maximize the S/N over the background. (Choosing an extraction radius of 2' does not change the spectral parameters quoted below). Redistribution matrix files (RMFs) and ancillary response files (ARFs) were generated using the SAS tasks *rmfgen* and *arfgen*, the latter in extended source mode. Appropriate flux-weighting was performed for RMFs, using our own dedicated software, and for ARFs, using exposure-corrected images of the source as detector maps (with pixel size of 1', the minimum scale modeled by *arfgen*) to sample the variation in emission, following the prescription of Saxton & Siddiqui (2002). The background was estimated locally using spectra extracted from a 2'-3' annular region positioned at the centroid of the emission; using a 3'-4' annulus gives results consistent within their 1σ errors. We checked that vignetting corrections for the sky background components do not affect the results by exploring the complementary approach of a complete modeling of the background components (including the thermal emission of NGC 5044) as in Gastaldello et al. (2006): the spectral results obtained are consistent with the ones quoted below within their 1σ errors.

The spectra from the three detectors were re-binned to ensure a signal-to-noise ratio of at least 3 and a minimum 20 counts per bin, and they were jointly fitted with an APEC thermal plasma modified by Galactic absorption (Dickey & Lockman 1990). The spectral fitting was performed with *Xspec* (ver11.3.1, Arnaud 1996) and quoted metallicities are relative to the abundances of Grevesse & Sauval (1998). We display the spectra in Fig.3. The source photons correspond to about 77% of the total events (~ 4400 counts in each MOS and ~ 7700 in the pn). An emission line is clearly visible corresponding to the Fe K α complex emitted at a redshift of $z = 0.27 \pm 0.01$. The redshift measured is in close agreement with the redshift of $z = 0.2814$ determined optically from the spectrum of the brightest cluster galaxy (see §3). Fixing the redshift value to the optical determination gives as best fit parameters, $T = 3.57 \pm 0.12$ keV, and, $Z = 0.60 \pm 0.09 Z_{\odot}$, for $\chi^2/\text{d.o.f.} = 486/463$.

Using the best-fit model, the unabsorbed flux within

the aperture of radius 1.5' (383 kpc) is $3.34_{-0.13}^{+0.08} \times 10^{-13}$ ergs cm $^{-2}$ s $^{-1}$ in the 0.5-2 keV band. This corresponds to an unabsorbed luminosity of $7.57_{-0.40}^{+0.10} \times 10^{43}$ ergs s $^{-1}$ in the 0.5-2 keV band and to a bolometric (0.01-100 keV) luminosity of $2.21_{-0.19}^{+0.34} \times 10^{44}$ ergs s $^{-1}$. The quoted errors on flux and luminosity are obtained by *Xspec* using a MonteCarlo procedure.

To investigate possible spatial variation in the spectral parameters of the cluster, we extracted two annular regions of radii 0'-0.5' and 0.5'-1.5'. The derived spectral parameters are: $T = 3.64 \pm 0.14$ keV and $Z = 0.66 \pm 0.13 Z_{\odot}$ with $\chi^2/\text{d.o.f.} = 280/231$ for the inner annulus; $T = 3.48_{-0.16}^{+0.19}$ keV and $Z = 0.52 \pm 0.13 Z_{\odot}$ with $\chi^2/\text{d.o.f.} = 280/271$ for the outer annulus. The width of the bins has been chosen in order to avoid bias in the temperature measurements caused by scattered flux by the PSF (80% encircled energy fraction radius is 25'' at 1.5 keV and at the off-axis angle of the source). The cluster is therefore consistent with being isothermal over the explored radial range.

XMMU J131359.7-162735 was also serendipitously detected in the *ROSAT* PSPC pointed observation of NGC 5044 (1WGA J1313.9-1627; White et al. 1994), though it was very close to the detector gaps. This is likely the reason why with *ROSAT* the source appeared not to be extended and had a lower flux ($1.75 \pm 0.14 \times 10^{-13}$ ergs cm $^{-2}$ s $^{-1}$ in the 0.2-2 keV band).

The cluster has regular X-ray isophotes and is centered on a dominant early type galaxy (see §3). These characteristics suggest the cluster is relaxed and that hydrostatic equilibrium is a good approximation. We calculated the total mass profile using two different models. First, we used the best-fit β model (see §2) for which the gas density and total mass profiles can be expressed by simple analytical formula (e.g., Ettori 2000). We evaluated r_{500} as the radius at which the density is 500 times the the critical density and the virial radius as the radius at which the density corresponds to Δ_{vir} , as obtained by Bryan & Norman (1998) for the concordance cosmological model used in this paper. To evaluate the errors on the estimated quantities, we repeat the measurements after 10000 random selections of a temperature and parameters of the surface brightness profile, which were drawn from Gaussian distributions with mean and variance in accordance with the best-fit results.

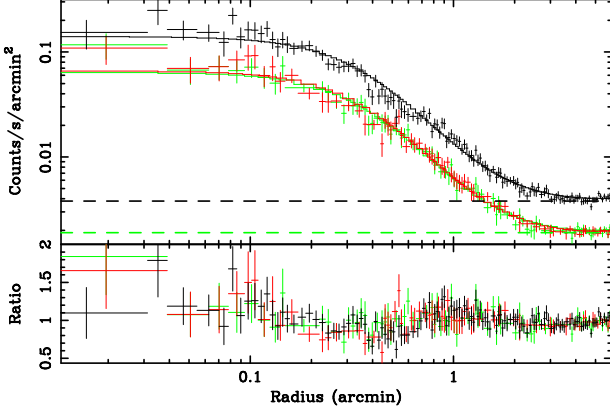


FIG. 2.— Surface brightness profile of the X-ray emission of XMMU J131359.7-162735. Data from MOS1, MOS2 and pn are plotted in green, red and black respectively. The best fit beta model and ratio of data over the model are also shown. The background level for PN and for one of the MOS are shown as black and green dashed lines respectively.

For $\Delta = 500$ we obtained, $M_{500} = (1.60 \pm 0.09) \times 10^{14} M_{\odot}$ within $r_{500} = 750 \pm 14$ kpc; the virial mass is, $M_{\text{vir}} = (3.24 \pm 0.18) \times 10^{14} M_{\odot}$, within the virial radius $r_{\text{vir}} = 1511 \pm 29$ kpc. Secondly, we fit the surface brightness profile with an isothermal NFW model (Suto et al. 1998). We obtain a concentration parameter, $c = 6.7 \pm 0.4$, virial radius $r_{\text{vir}} = 1607^{+48}_{-42}$ kpc, and virial mass $M_{\text{vir}} = (3.89 \pm 0.35) \times 10^{14} M_{\odot}$, with $\chi^2/\text{d.o.f.} = 424/273$. The mass determinations using the two different models are in agreement within the 1σ errors.

3. OPTICAL FOLLOW-UP OBSERVATIONS

A V -band and I -band image of the field were taken with the direct imaging CCD on the 2.5-m du Pont Telescope at Las Campanas Observatory on the night of 27 January 2006. In both wavebands, 2×300 s exposures were taken in clear, photometric conditions. Photometric zero-points and extinction corrections were determined by observing three standard stars chosen from the Landolt (1992) catalog. The images have been processed and cleaned of CCD defects and cosmic rays. The V -band image is shown with X-ray contours superposed in Fig.1. The image reveals an over-density of galaxies and, in particular, a bright dominant galaxy at the same location as the X-ray centroid.

Photometry was performed using SExtractor (Bertin & Arnouts 1996) with automatic aperture magnitudes. We plot in the top panel of Fig.4 the color-magnitude diagram of the galaxies detected within $3.1'$ radius of the central galaxy (corresponding to 803 kpc, half of the estimated virial radius): the horizontal dashed line corresponds to the expected $V - I$ color of a passively evolving elliptical galaxy at $z \sim 0.28$, which is $V - I \sim 1.6$ for a formation redshift, $z > 5$ (Nelson et al. 2002). The difference in magnitude between the central galaxy ($m_I = 16.4$) and the likely cluster members is very close to the 2 magnitudes of the definition of fossil systems (Jones et al. 2003). We have excluded three objects (triangles in Fig.4) because they are likely members of the NGC 5044 group. A further two objects, which are within 2 magnitudes of the BCG, are very far

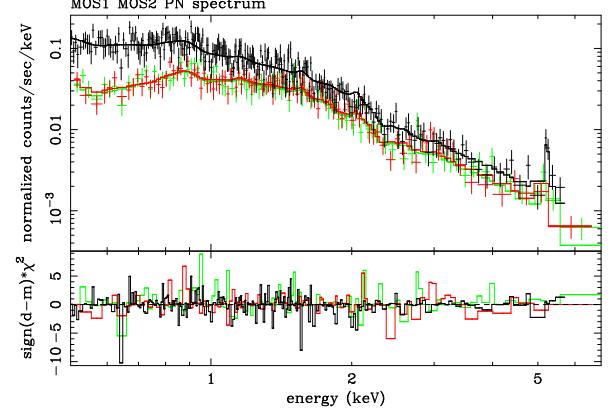


FIG. 3.— X-ray spectrum of the source taken from a $1.5'$ aperture positioned at the centroid of the emission. Data from MOS1, MOS2 and pn are plotted in green, red and black respectively. The best fit model and residuals are also shown.

from the cluster center ($2.6'$, 664 kpc, and $2.5'$, 638 kpc, crosses in Fig.4). A possible member is 1.9 magnitudes fainter than the BCG at a distance of $1.8'$ (diamond in Fig.4).

We obtained an optical spectrum of the central galaxy on the night of 7 March 2006 UT, using the ESI spectrograph (Sheinis et al. 2002) at the Keck-II telescope. A $0.75''$ slit width was used, giving a spectral resolution of $\sim 50 \text{ km s}^{-1}$ (FWHM) and a pixel scale of $11.4 \text{ km s}^{-1} \text{ pixel}^{-1}$. The galaxy was observed at airmass 1.25 for 900 s in partly cloudy conditions, and the slit was oriented at the parallactic angle. The spectrum was extracted with a $1''$ extraction width, and wavelength calibrated and flux-calibrated using an observation of the standard star Feige 34. The individual echelle orders were combined into a single spectrum. The galaxy redshift was measured by performing a direct fit of a K3III stellar spectrum (observed on the same night with ESI), velocity-broadened by convolution with a Gaussian kernel. The best-fitting model yields a recession velocity of $84360 \pm 19 \text{ km s}^{-1}$, or $z = 0.2814 \pm 0.0001$, in close agreement with the redshift estimated from the X-ray observations. The ESI spectrum is shown in the bottom panel of Fig.4.

4. DISCUSSION

This serendipitously discovered cluster obeys the scaling relations for L_X and T derived at intermediate redshift. The aperture of 383 kpc used for spectroscopy encloses 78.3% of the flux within r_{500} , assuming the cluster emission profile follows the β model derived within that aperture. The derived bolometric luminosity within r_{500} is $L_{500} = (2.82^{+0.43}_{-0.24}) \times 10^{44} \text{ ergs s}^{-1}$. The derived L_{500} is in good agreement with the $L - T$ relation found for the sample of low redshift clusters ($z < 0.09$) by Markevitch (1998), the low-redshift groups ($z < 0.03$) in the GEMS sample (Osmond & Ponman 2004), the six groups/poor clusters at intermediate redshift ($0.29 < z < 0.44$) in the *XMM* LSS survey (Willis et al. 2005), and the six groups/poor clusters at intermediate redshift ($0.23 < z < 0.59$) in the sample of Jeltema et al. (2006).

The optical appearance of the cluster suggests tantalizing evidence that this object may be one of the rare fossil clusters (3%-6% of the total number according to Milosavljević et al. 2006). More detailed optical imaging

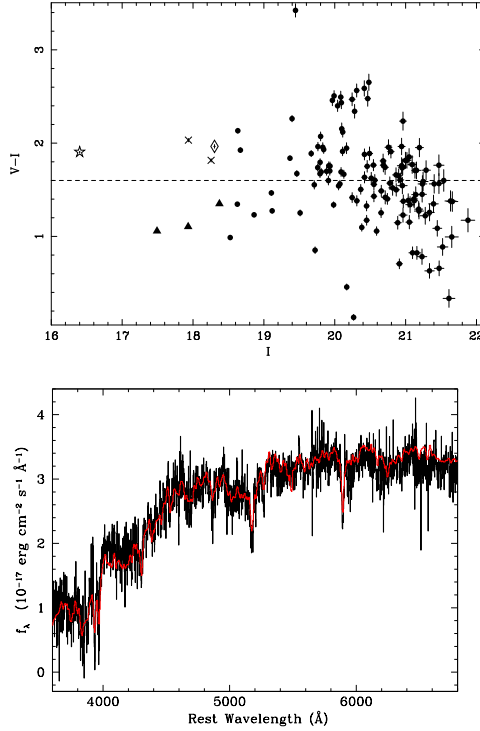


FIG. 4.— *Top*: Color-magnitude diagram of the galaxies within $2.8'$ of XMMU J131359.7–162735. The horizontal dashed line indicates the predicted color of a $z = 0.28$ cluster elliptical. The star indicates the BCG. Triangles indicate likely dwarf members of NGC 5044 (one of them is the object #26 in the catalog of Ferguson & Sandage 1990). Crosses indicate objects very far from the BCG (see text). The diamond indicates the only other object within 2 magnitudes of the BGC. *Bottom*: A portion of the Keck ESI spectrum, binned to $2 \text{ Å}/\text{pixel}$. Over-plotted in red is the elliptical galaxy template spectrum from the spectral atlas of Kinney et al. (1996).

and spectroscopy are required to investigate this possibility. The derived total magnitude for the BCG, corrected

for Galactic extinction, as well as for the k -correction (Fukugita et al. 1995), is $M_I = -24.78$, which corresponds to $M_B = -22.38$ and $M_R = -24.05$, adopting colors $B - I_J = 2.40$ and $R_J - I_J = 0.73$ (Fukugita et al. 1995). The BCG of XMMU J131359.7–162735 is among the most luminous in the sample of BCGs in fossil systems of Khosroshahi et al. (2006). The measured values of L_B of the BCG and L_X put the object very close to the locus of baryonic closure (Mathews et al. 2005), as expected for fossil systems.

The measured c , multiplied by the expected dependence of $1 + z$ (Bullock et al. 2001), is consistent with a ΛCDM model with $\sigma_8 = 0.9$ indicative of a relaxed, early forming system in agreement with the theoretical prediction for fossil systems (Zentner et al. 2005; D’Onghia et al. 2005) and with the observational results of relaxed, low- z clusters (Buote et al. 2006).

5. CONCLUSIONS

The discovery of XMMU J131359.7–162735 reported in this letter represents the deepest observation among the intermediate redshift systems discussed in the literature (Willis et al. 2005; Jeltema et al. 2006), and it already provides an interesting description of its fundamental parameters and dynamical state. Future optical spectroscopy and dedicated X-ray follow-up will allow detailed spectral properties to be measured.

We thank the referee, H. Ebeling, for useful comments and suggestions. Partial support for this work was provided by NASA-XMM grant NNG06GC48G. The authors wish to acknowledge the very significant cultural role and reverence that the summit of Mauna Kea has always had within the indigenous Hawaiian community. We are most fortunate to have the opportunity to conduct observations from this mountain.

REFERENCES

- Arnaud, K. A. 1996, in ASP Conf. Ser. 101: Astronomical Data Analysis Software and Systems V, Vol. 5, 17
- Bertin, E. & Arnouts, S. 1996, A&AS, 117, 393
- Bryan, G. L. & Norman, M. L. 1998, ApJ, 495, 80
- Bullock, J. S., Kolatt, T. S., Sigad, Y., Somerville, R. S., Kravtsov, A. V., Klypin, A. A., Primack, J. R., & Dekel, A. 2001, MNRAS, 321, 559
- Buote, D. A., Gastaldello, F., Humphrey, P. J., Zappacosta, L., Bullock, J., Brighenti, F., & Mathews, W. 2006, ApJ, submitted, (astro-ph/0610135)
- Buote, D. A., Lewis, A. D., Brighenti, F., & Mathews, W. G. 2003, ApJ, 594, 741
- Cavaliere, A. & Fusco-Femiano, R. 1978, A&A, 70, 677
- Dickey, J. M. & Lockman, F. J. 1990, ARA&A, 28, 215
- D’Onghia, E., Sommer-Larsen, J., Romeo, A. D., Burkert, A., Pedersen, K., Portinari, L., & Rasmussen, J. 2005, ApJ, 630, L109
- Ettori, S. 2000, MNRAS, 311, 313
- Ferguson, H. C. & Sandage, A. 1990, AJ, 100, 1
- Fukugita, M., Shimasaku, K., & Ichikawa, T. 1995, PASP, 107, 945
- Gastaldello, F., Buote, D. A., Humphrey, P. J., Zappacosta, L., Bullock, J. S., Brighenti, F., & Mathews, W. G. 2006, ArXiv Astrophysics e-prints, ApJ, submitted (astro-ph/0610134)
- Grevesse, N. & Sauval, A. J. 1998, Space Science Reviews, 85, 161
- Jeltema, T. E., Mulchaey, J. S., Lubin, L. M., Rosati, P., & Böhringer, H. 2006, ApJ, 649, 649
- Jones, L. R., Ponman, T. J., Horton, A., Babul, A., Ebeling, H., & Burke, D. J. 2003, MNRAS, 343, 627
- Khosroshahi, H. G., Ponman, T. J., & Jones, L. R. 2006, MNRAS, 372, L68
- Kinney, A. L., Calzetti, D., Bohlin, R. C., McQuade, K., Storchi-Bergmann, T., & Schmitt, H. R. 1996, ApJ, 467, 38
- Landolt, A. U. 1992, AJ, 104, 340
- Markevitch, M. 1998, ApJ, 504, 27
- Mathews, W. G., Faltenbacher, A., Brighenti, F., & Buote, D. A. 2005, ApJ, 634, L137
- Milosavljević, M., Miller, C. J., Furlanetto, S. R., & Cooray, A. 2006, ApJ, 637, L9
- Mulchaey, J. S., Lubin, L. M., Fassnacht, C., Rosati, P., & Jeltema, T. E. 2006, ApJ, 646, 133
- Nelson, A. E., Gonzalez, A. H., Zaritsky, D., & Dalcanton, J. J. 2002, ApJ, 566, 103
- Osmond, J. P. F. & Ponman, T. J. 2004, MNRAS, 350, 1511
- Pierre, M., et al. 2004, Journal of Cosmology and Astro-Particle Physics, 9, 11
- Saxton, R. D. & Siddiqui, H. 2002, XMM-SOC-PS-TN-43
- Sheinis, A. I., Bolte, M., Epps, H. W., Kibrick, R. I., Miller, J. S., Radovan, M. V., Bigelow, B. C., & Sutin, B. M. 2002, PASP, 114, 851
- Suto, Y., Sasaki, S., & Makino, N. 1998, ApJ, 509, 544
- Voit, G. M. 2005, Rev. Mod. Phys., 77, 207
- White, N. E., Giommi, P., & Angelini, L. 1994, IAU Circ., 6100, 1
- Willis, J. P., et al. 2005, MNRAS, 363, 675

Zentner, A. R., Berlind, A. A., Bullock, J. S., Kravtsov, A. V., &
Wechsler, R. H. 2005, ApJ, 624, 505